# WHEN LESS IS MORE: EXPERIMENTAL EVIDENCE FOR TENACITY ENHANCEMENT BY DIVISION OF CONTACT AREA

Andrei Peressadko[a]; Stanislav N. Gorb[a]

[a] Evolutionary Biomaterials Group, Heisenbergstr, Stuttgart, Germany

## PLEASE SCROLL DOWN FOR ARTICLE

Taylor & Francis
Taylor & Francis Group

# WHEN LESS IS MORE: EXPERIMENTAL EVIDENCE FOR TENACITY ENHANCEMENT BY DIVISION OF CONTACT AREA

**Andrei Peressadko**
**Stanislav N. Gorb**
Evolutionary Biomaterials Group,
Max-Planck-Institut für Metallforschung,
Heisenbergstr, Stuttgart, Germany

*Most recent data on hairy systems demonstrated their excellent adhesion and high reliability of contact. In contrast to smooth systems, some hairy systems seem to operate with dry adhesion and do not require supplementary fluids in the contact area. Contacting surfaces in such devices are subdivided into patterns of micro- or nanostructures with a high aspect ratio (setae, hairs, pins). The size of single points gets smaller and their density gets higher as the body mass increases. Previous authors explained this general trend by applying the JKR theory, according to which splitting up the contact into finer subcontacts increases adhesion. Fundamental importance of contact splitting for adhesion on smooth and rough substrata has been previously explained by a very small effective elastic modulus of the fibre array. This article provides the first experimental evidence of adhesion enhancement by division of contact area. A patterned surface made out of polyvinylsiloxane (PVS) has significantly higher adhesion on a glass surface than a smooth sample made out of the same material. This effect is even more pronounced on curved substrata. An additional advantage of patterned surfaces is the reliability of contact on various surface profiles and the increased tolerance to defects of individual contacts.*

Many animals bear leg attachment pads with an excellent ability to adhere to a smooth surface as well as to a variety of natural surfaces with rough profiles. There are two alternative designs of such systems: smooth and hairy [1]. The first type of pads, so-called smooth systems such as arolia and euplantulae, occurs in cockroaches, bees, grasshoppers, and bugs, are soft deformable structures with a relatively smooth surface [2]. Pads of geckos, flies, beetles, and spiders are covered by relatively long, deformable setae (Figure 1) that, due to individual bending, increase the number of contacting points with the surface.

Most recent data on hairy systems demonstrated their excellent adhesion and high reliability of contact [3, 4]. In contrast to smooth systems, some hairy systems seem to operate because of dry adhesion and do not require supplementary fluids in the contact area [5, 6]. Interestingly, hairy systems appeared several times in animal evolution and at least three times independently even within insect evolution. This fact may indicate that such a design of surfaces must have an advantage for adhesion enhancement not only in biological systems but also on artificial surfaces. The physical background of this effect was theoretically discussed in several recent publications [7, 8].

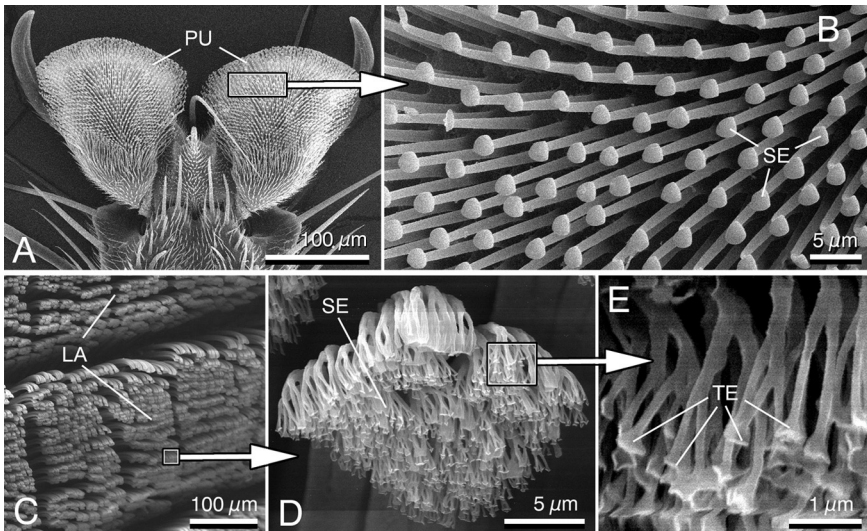

**FIGURE 1** Biological attachment surfaces, scanning electron microscopy. (a)–(b). Pads (pulvilli) of the leg of the fly *Episyrphus balteatus* are divided into setae with flat tips. (c)–(e). Pads of the leg of the gecko *Gecko gekko* consist of lamellae, which are subdivided into setae branching into even finer terminal elements. LA, lamellae; PU, pulvilli; SE, setae; TE, terminal elements.

Comparison of a wide variety of animal groups revealed that the size of single contacting points gets smaller and their density increases as the body mass increases [9]. This general trend is theoretically explained by applying the Johnson-Kenndall-Roberts (JKR) theory, according to which splitting up the contact into finer subcontacts increases adhesion [10]. The effective elastic modulus of the fiber arrays is very small, which is of fundamental importance for adhesion on smooth and rough substrata [8]. It is predicted that an additional advantage of patterned surfaces is the reliability of contact on various surface profiles and the increased tolerance of defects at individual contacts. In a real situation, failure of some microcontacts due to dust particles or to mechanical damage of single seta would minimally influence contact adhesion. In the case of a solitary contact, even slight damage of the contact due to the presence of dirt or surface irregularities will immediately lead to contact breakage similar to the crack propagation in bulk material.

However, these theoretical considerations were not proven experimentally. In this study, adhesion of the structured surface on a smooth glass surface was compared with the adhesion of a flat sample made out of the same bulk material. The JKR theory was applied to model behaviour of the single contact. This article provides the first experimental evidence of adhesion enhancement by division of contact area. Additionally, it is shown that this effect is even more pronounced on curved substrata.

## THEORY

Adhesion energy of the contact between two bodies 1 and 2 can be expressed as

$$W_a = w_{12}S_{12} \tag{1}$$

where $W_{12}$ is specific adhesion energy of the contacting surfaces in $J/m^2$ and $S_{12}$ is the area of the adhesion contact $(m^2)$ [11]. Note that the area of adhesion contact $(S_{12})$ is considerably smaller than the apparent or geometrical contact area $S_{geom}$: $S_{12} << S_{geom}$. For metals, the relationship between both areas is evaluated as approximately $1/10000$ [12]. Specific energy of the adhesion contact, $W_{12}$, is determined by the physical and chemical properties of contacting materials. Contacting area, $S_{12}$, depends on the profile of surfaces and mechanical properties of both materials. Thus, it can be concluded from Equation (1) that adhesive energy, $W_a$, depends on two variables—specific energy of the adhesion, $W_{12}$, and contact area of surfaces, $S_{12}$. Transition

from the adhesion energy, $W_a$, to the adhesion force, $F_a$, is a nontrivial problem solved analytically only for some ideal cases. The most prominent case of the solution is the JKR model [13] based on the Hertz model [14], which considers contact of two ideally smooth spheres. The JKR model considers the Hertz contact, taking into account the influence of attractive force. Radius of the contact area, $a$, in the JKR theory depends on the radii of both spheres, $R_1$ and $R_2$, elasticity modulus of both materials, $E_1$ and $E_2$ the specific energy of contacting surfaces, $w$, and the load/adhesion force, $P$:

$$a^3 = \frac{3R}{4E^*}\left(P + 3w\pi R + \sqrt{6w\pi RP + (3w\pi R)^2}\right), \qquad (2)$$

where $R = (1/R_1 + 1/R_2)^{-1}$ is the reduced radius and $E^* = \left((1 - v_1^2)/E_1 + 1 - (v_2^2)/E_2\right)^{-1}$ is the reduced elasticity modulus.

The pull-off force, $P$, of the sphere with the radius, $R$, from the plane with the adhesion energy, $w$, is expressed in the JKR theory as

$$P = -\frac{3}{2}\pi wR. \qquad (3)$$

For a flat surface with a large radius of curvature when $R_2 >> R_1$, it may be suggested that $R \cong R_1$.

## MATERIALS AND METHODS

### Sample Geometry

The structured sample had a total dimension of $2.12 \times 2.75\,mm$ and consisted of 72 pins (ten rows with about seven pins in each) ( Figure 2a and 2b). Pin height was about $L = 0.4\,mm$ (Figures 2c and 2d). In the cross section $l \times B$, each pin was $\sim 0.250 \times 0.125\,mm$. Total geometrical area of structured sample was $S_{struct.\,geom.} = 5.83\,mm^2$. For control experiments, a polyvinylsiloxane (PVS) mould of the smooth glass surface ($R_a = 0.5\,nm$) of an area ($S_{flat\,geom.}$) of $14.6\,mm^2$ was used.

The samples were obtained by moulding of the template with a two-compound polymer polyvinylsiloxane (PVS) (President® light body, Coltene, Switzerland). The template for a structured sample was made as a pattern of oval-shaped holes $\sim 0.2 \times 0.1\,mm$ in size. The holes were burned through a stainless steel plate 0.4 mm thick. The template was made by Lasertechnik Thiringer GmbH (Oberndorf, Germany). Polymer, in its fluid condition, flows into finite valleys of the surface and, after polymerisation, perfectly casts the surface and
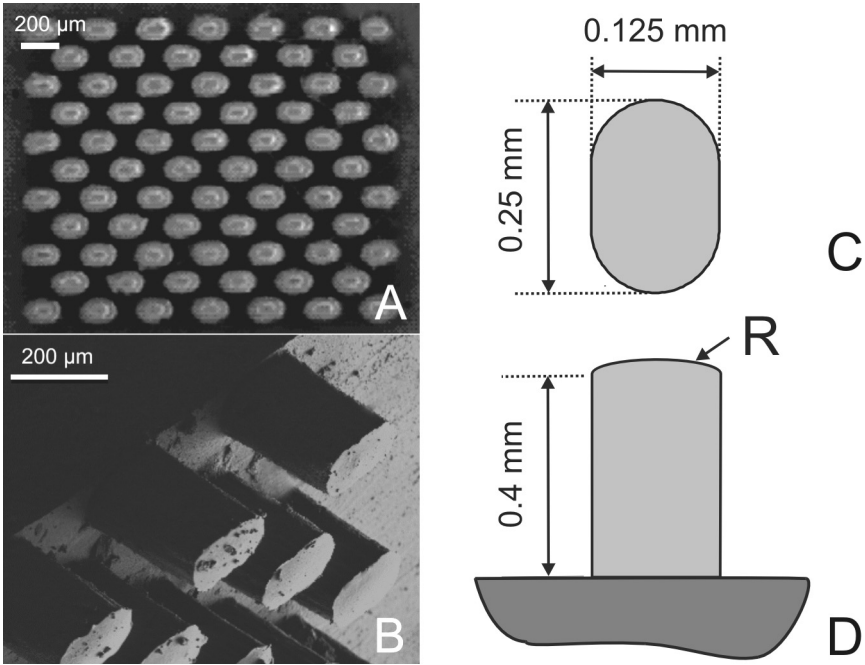
**FIGURE 2** Structured sample made out of PVS. (a) Entire sample viewed from above under binocular microscope. (b) Single pins of the sample, micrograph obtained by Finite Ion Beam (FIB). (c)–(d) Dimensions of the single pin.

can be easily separated from the template [9]. Thickness of the PVS base underlying pins was approximately 3 mm.

Depending on the pressure applied to the fluid mixture of components prior to polymerisation, various pin tips may be obtained: (1) convex with a positive radius of curvature ($R_{curv} > 0$), (2) concave with a negative radius of curvature ($R_{curv} < 0$), and (3) flat ($R_{curv} = 0$). Samples with low radii of curvature of the pin surface $R = \pm 0.1 - 1$ mm had low adhesive abilities; only samples with a pin surface with curvature larger than $4 - 5$ mm were selected for experiments. Radius of curvature of the pin tips was inspected by the use of the white-light interferometer Zygo New View 5000 (Zygo Corporation, Middlefield, CT, USA). Most of the samples had pin tips of elliptic shape with various radii of curvature in the longitudinal and transversal directions. When the difference between these radii is low, such an elliptical surface can be described by a sphere with a radius of $R = \sqrt{R_{long} R_{cross}}$, and the JKR theory can be applied to model the contact between pin tip and flat surface.

## Properties of the Bulk Material of the Sample

Young's modulus of the bulk material ($E$) was determined by microindentation [15] of the flat surface by a sapphire sphere having a diameter ($D$) of 0.5 mm and calculated according to the JKR theory [13]. Young's modulus ranged from 2.5 to 3 MPa.

Surface energy of the PVS was calculated from contact angles of distilled water, diiodomethane, and ethylene glycol by the use of a contact angle measurement device OCA-20 (Dataphysics GmbH, Fielderstadt, Germany). PVS is a highly hydrophobic material. The contact angle ($\Theta$) of distilled water on its surface was $112°$. Surface energy of PVS ($\gamma$) was $16.1 \, \mathrm{mJ/m^2}$ ($\gamma_d = 13.1 \, \mathrm{mJ/m^2}$ -dispersion part, $\gamma_p = 3 \, \mathrm{mJ/m^2}$ -polar part) according to the method Wu implemented in the OCA-20 contact angle measurement device.

## Adhesion Measurements

Adhesion of smooth and structured PVS samples was measured on glass surfaces. The glass sample was immobile. The PVS sample was firmly glued to the glass plate, attached to the load cell force transducer FORT 100 (World Precision Instrument Inc., Sarasota, FL, USA). The whole sample was mounted to a three-axial motorized micromanipulator DC3001 (World Precision Instrument Inc., FL) controlled with stepper motors moving with a velocity of $200 \, \mu m/s$. The PVS sample was oriented parallel to the glass surface and both surfaces were perpendicular to the load direction. The sample was brought into contact and detached by linear motion of the manipulator, which was perpendicular to the glass surface (Figure 3). The glass sample was loaded with the PVS sample. The load ranged from 0.1 to 1000 mN. Adhesion was measured during unloading (Figure 3). The contact area was videorecorded in each cycle of the load in the light reflection mode by using an optical microscope Leica MZ12.5 with a built-in video camera. The contact area was measured from digitised single frames with the SigmaScan Pro 5 software (SPSS). We called this contact *measured contact area*. Of course, it is not the same as the real contact, where the two solids are in atomic contact at the interface. Measured contact area is almost always larger than the real contact area.

Two series of experiments with structured and flat PVS (control) samples were carried out. In the first series, adhesion of both samples was measured in contact with the flat glass sample (roughness $R_a = 0.5 \, \mathrm{nm}$, surface energy $\gamma_g = 53.2 \, \mathrm{mJ/m^2}$, dispersion fraction of the surface energy $\gamma_d = 27.4 \, \mathrm{mJ/m^2}$, polar fraction of the surface
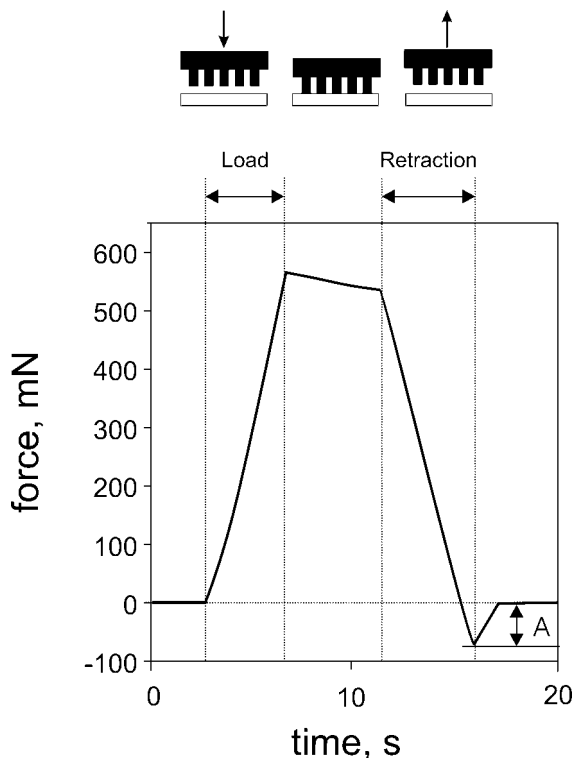
**FIGURE 3** Typical force curve obtained in adhesion experiments. A, adhesion; *Load*, loading part of the curve; *Retraction*, unloading part of the curve.

energy $\gamma_p = 25.8\,\text{mJ/m}^2$). In order to evaluate the influence of the substrate curvature on the adhesion of both PVS samples, in the second series, the adhesion was measured on the convex surface of glass cylinders of various diameters (5, 10, 20, 40, 55, and 80 mm). In the second experiment, contact area between samples was not determined.

## RESULTS

### Adhesion of PVS Samples on a Flat Glass Surface

For the structured PVS sample, absolute values of measured adhesion ranged from 20 to 40 mN at loads $< 150\,\text{mN}$ and reached 60 mN at loads ranging from 150 to 400 mN (Figure 4). At the mean adhesion

**FIGURE 4** Adhesion of structured and flat samples on the flat glass surfaces. Insets show profiles of the pin shape at different loads.

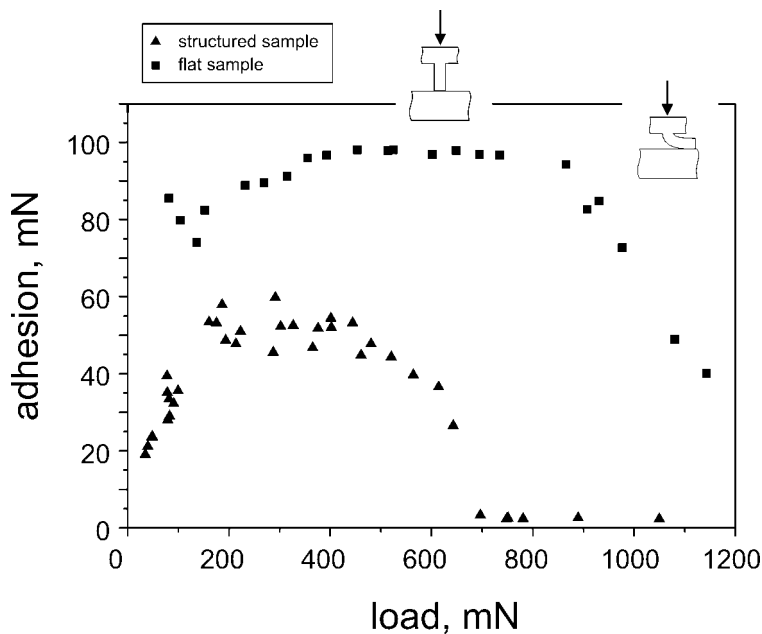force of the entire sample of $F_\Sigma = 40.02$ mN, adhesion force of the single pin was about $F_{pin} = 0.56$ mN. At higher loads (600–650 mN), adhesion dropped to 0. Such a sudden drop in the adhesion force is due to buckling of pins. At very high loads, the pins buckle: they fall on their side and no longer touch the glass surface with their tips.

Experimentally determined contact area of structured and flat PVS samples on glass varies depending on the load applied to the sample (Figures 5d and 5e). The increase in the load from 0.1 to 300 mN results in an increase of the contact area from 0.05 mm$^2$ to 1.70 mm$^2$. Higher contact areas (1.7–2.0 mm$^2$) correspond to higher loads (300–600 mN). Further increase in the load results in pin buckling (Figure 5c). This may further increase the contact area, because the sides of the pins contact the glass surface (Figure 5d). As the buckling pins start to contribute to the total contact area between both samples, adhesion tends to decrease. For the structured PVS sample, a load range of 600–650 mN may be determined as load limit or buckling load at which almost zero adhesion was measured. Thus, such an increase in the contact area does not influence adhesion
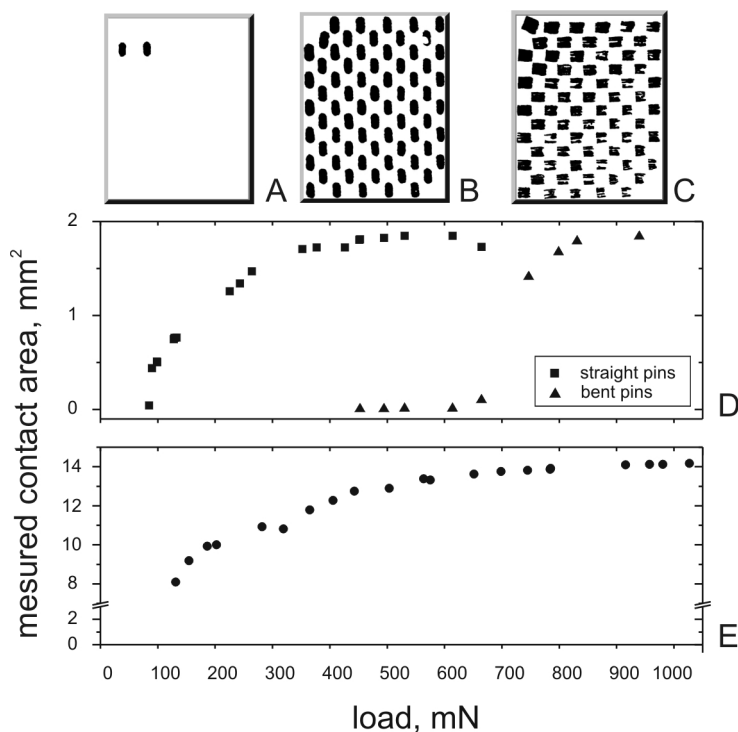
**FIGURE 5** (a)–(c) Contact area of the structured sample in the reflecting light under binocular microscope. Note that pins are buckled in (c). Dependence of the contact area of the (d) structured and (e) flat PVS samples on load. Contact areas of straight buckled pins are given separately (d).

(Figure 4), because of the high amount of elastic energy stored in the deformed pins.

For the flat PVS sample, measured adhesion ranged from 80 to 100 mN at loads of 50–850 mN. Mean adhesion force at loads of 150–500 mN was 95.6 mN. At loads > 850 mN, adhesion forces tended to decrease. Measured contact area of the flat sample increased from 8 mm$^2$ at a load of 120 mN and asymptotically approaches the value of 14 mm$^2$ when the load increases (Figure 5e).

To compare adhesive properties of the structured and flat samples, the tenacity (adhesion per unit of measured contact area) was calculated for both samples (Figure 6). The structured surface has 2–4 times higher tenacity at loads under the buckling load. Average tenacity at loads of 100–500 mN was $7.89 \pm 0.43$ mN/mm$^2$ for the flat PVS sample and $32.4 \pm 5.71$ mN/mm$^2$ for the structured one
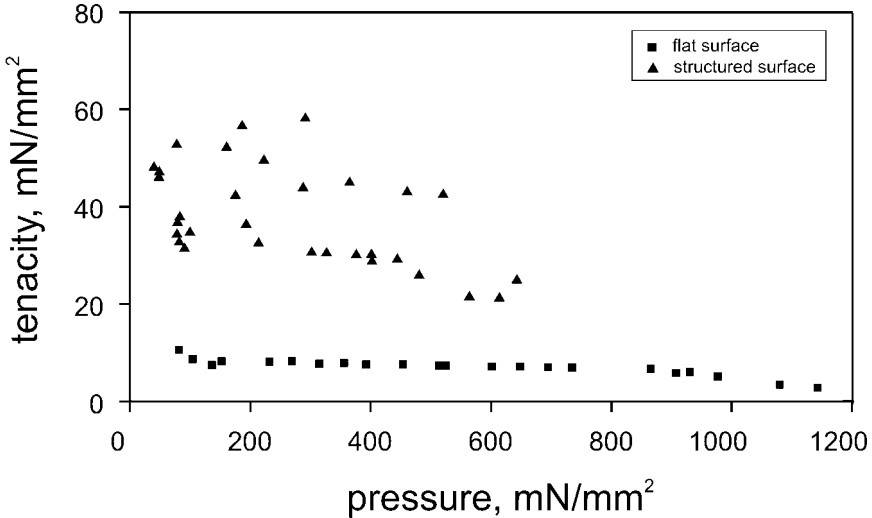
**FIGURE 6** Dependence of tenacity of the structured and flat samples on the pressure.

(Figure 6). Adhesive force per unit total geometrical area gives, for the structured sample, $40.2 \, \text{mN}/5.83 \, \text{mm}^2 = 6.9 \, \text{mN/mm}^2$, and for the flat sample $95.6 \, \text{mN}/14.6 \, \text{mm}^2 = 6.5 \, \text{mN/mm}^2$.

## Adhesion of Samples to Curved Surfaces

At high ( $> 120 \, \text{m}^{-1}$) and low ($< 40 \, \text{m}^{-1}$) curvatures of the glass surface, adhesion of the flat PVS sample was much higher than that of the structured sample. At intermediate curvatures of the glass surface ($40-120 \, \text{m}^{-1}$), adhesion of the structured PVS sample was considerably higher (Figure 7).

## DISCUSSION

## Why do Structured Surfaces Stick Better?

Above results demonstrate that surface structuring has two main effects on adhesion: (1) it leads to an increase of the tenacity (adhesion per unit of the measured contact area) of the surface and (2) it improves the surface if ability to attach to nonplanar surfaces.

The average radius of a pin tip was about $R = 5 \, \text{mm}$, and specific energy of adhesion (SAE) is $w_{12} = 2\sqrt{\gamma_1 \gamma_2} = 2\sqrt{16.1 \cdot 53.2} = 58.5 \, \text{mN/m}$
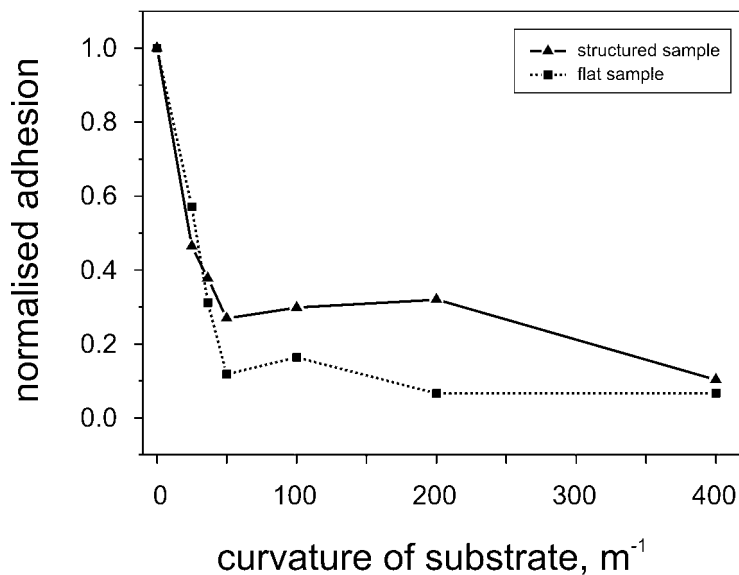
**FIGURE 7** Dependence of adhesion of the structured and flat samples on the curvature of the glass substrate. Adhesion is normalised to the adhesion on the flat glass substrate.

[16]. Let us consider adhesion force of such a pin according to the JKR theory:

$$F_{\text{pull-off}} = -\frac{3}{2}\pi w_{12}R = -1.38\,\text{mN}.$$

Adhesion force obtained from such a calculation ($1.38\,\text{mN} \times 72$ pins = $99.36\,\text{mN}$) is more than two times higher than adhesion force obtained in the experiment ($40.02\,\text{mN}$). This difference may be explained by the slightly nonparallel orientation of both flat samples and somewhat different lengths of pins. A not ideally parallel orientation of samples may result in nonsimultaneous separation of pins from the glass surface. Additionally, it may be suggested that not all pins were in intimate contact with the glass surface. If we assume that adhesion corresponds to the JKR theory, we can calculate the number of pins having intimate contact with the glass surface ($40.02/99.36 \cdot 100\% \cong 40\%$). Thus, only less than one-half of the pins were in contact with their counterpart and contributed to the overall adhesion of the sample.

Our experiment demonstrated that single pins of the structured surface buckle at a certain load. The buckling load of the single pin

is related to the moment of inertia ($J$) of the pin and elastic modulus of the material [17]. Minimal moment of inertia of the pin is $J = 5.27 \times 10^{-17}$ m$^3$. Total theoretical buckling load of the pin pattern estimated by the Euler formula gives a value of 630 mN.

The structured sample (Figure 7) demonstrated even higher normalized adhesion forces ($F_{adh}/F_{adh\,max}$) while in contact with the curved surface at curvatures ranging from 40 to 120 m$^{-1}$. Presumably, this range of curvatures depends on the pin size (length $- l$, width $- b$, and the cross section) as well as on the mechanical properties of the pin material (Young's modulus, $E$, Poisson's ratio, $\mu$). However, the relationship between these variables cannot be obtained from available data.

We obtained an apparently paradoxical result—tenacity of the structured surface is higher than that of the flat sample. In other words, unit contact area of the structured sample generates comparatively higher adhesion force than that of the flat sample (Figure 6). Since adhesion energy between PVS and glass does not change depending on the surface geometry, one may presume that the structured surface has a higher real contact area with the substrate at a lower measured contact area and a lower amount of stored elastic energy than the flat sample. Both effects will result in better adhesive properties of the structured material.

Why does the structured surface stick better to glass? The effectiveness of the attachment system may be evaluated through the energy. Contact energy (Equation (4)) is the difference between adhesion energy $W_{adhesion}$ and elastic energy $W_{elastic}$ stored in the contact:

$$W_{contact} = W_{adhesion} - W_{elastic}. \tag{4}$$

The structured sample has lower surface rigidity and thus higher flexibility. This increases the ability of the surface to adapt to the substrate irregularities in contrast to the flat sample. The flat sample is able to build contact only at the tips of substrate irregularities and, therefore, generate only rather low real contact area. Thus, one may formulate an ultimate requirement for an effective attachment system — *the system must reach maximal contact energy at the minimal elastic energy spent for formation of the contact area*.

## Two Ways to Enhance Sticking Ability of Surfaces

Let us consider Equation (1) for the highest adhesion in the system, $W_{contact}$, for which many attachment–detachment cycles are required. There are two ways to increase adhesion energy of the contact ($W_a$). The first is to increase the specific adhesion energy SAE ($w_{12}$) at

constant contact area ($S_{12} = const$). The second is to increase real contact area ($S_{12}$) at constant SAE ($W_{12} = const$).

The first way has some limitations. Maximal SAE has limited ranges from $50-70 \, \text{mJ/m}^2$ in glass, silicon, and GaAs, and, $300-400 \, \text{mJ/m}^2$ in metals. Additionally, a high SAE results in the rather fast passivity of the surface even under normal conditions. For example, the SAE of mica cleaned in a high vacuum is $\gamma_s \approx 4500 \, \text{mJ/m}^2$, whereas the SAE of mica cleaned in atmospheric conditions is $\gamma_{sv} \approx 300 \, \text{mJ/m}^2$ [16]. Thus, under natural conditions, in the presence of humidity, various gases, and dust, the surface with high SAE will be contaminated very quickly and its SAE will be rapidly dropped, effecting a decrease of the surface stickiness.

The adhesion energy of the contact ($W_{contact}$) may also be enhanced by the second way, namely by an increase of the real contact area between two surfaces. As mentioned above, the relationship between real contact area and geometrical contact area in metals is about $1/10000$ [12], and it mainly depends on the surface geometry. Presumably, this relationship is similar for stiff materials. Surface patterning into structures with a high aspect ratio results in an increase of the real contact area between two surfaces and in the enhancement of adhesion energy of the contact. A lower stiffness of the structured surface results in a higher deformability of the surface and, therefore, in a higher ability to build areas of real contact with any surface. A structured surface has a lower portion of elastic energy stored in the material. Such a decrease of the stored elastic energy of deformation, $W_{elastic}$, results in an increase of the adhesion energy, $W_{adhesion}$. This way does not have the disadvantages mentioned above for the first way. The area of real contact may be widely varied depending on the load applied and is less dependent on contamination than the SAE.

## Applications to Biological Attachment Devices

From our studies on biological adhesive systems, such as attachment pads of geckos, flies, beetles, and spiders (Figure 1), one may conclude that they are designed according to the second way of enhancement of the sticking ability [1, 9, 18]. Multiple contacts of the attachment pads have two advantages for adhesion enhancement: (1) increase of the real contact area on fractal profiles of natural surfaces and (2) decrease of the elastic energy storage [8]. A very coarse evaluation of the maximum adhesion of the gecko pad, if all setae are in contact with a flat surface, gives a value of $1300 \, \text{N}$ [6, 8] for animals weighing $1-2 \, \text{N}$ [4]. However, the maximum force measured for one pad is about $10 \, \text{N}$ [4]. Thus, only about $2/1300 \times 100\% \cong 0.15\%$ of the total amount

of setae of one pad are sufficient to hold the body on the ceiling. About $(4 \times 10)/1300 \times 100\% \cong 3\%$ of setae of one pad are simultaneously in contact. These data led the authors to conclude that the hairy attachment system of the gecko has certain superfluity, which leads to an increase of the contact reliability on surfaces with various profiles.

## CONCLUSIONS

Contacting surfaces in the majority of biological attachment devices are subdivided into patterns of micro- or nanostructures with a high aspect ratio (setae, hairs, pins). The most important property of such a system is the enhancement of the adhesion energy of the contact by an increase of real contact area at the constant surface energy of material. Only about 0.15% of setae of the gecko pad system are required to reach sufficient adhesion to hold the body on the ceiling. This article provides the first experimental evidence of the adhesion enhancement by division of contact area. It is shown that this effect is even more pronounced on curved substrata. The excess of pins in biological systems, as well as in the patterned surface described here, guarantees the stability of the contact and provides adaptation to various surface profiles.

## REFERENCES

[1] Gorb, S. N., *Attachment Devices of Insect Cuticle*. (Kluwer Academic Publishers, Dordrecht, Boston, London, 2001).

[2] Jiao, Y., Gorb, S. N., and Scherge, M., Adhesion measured on the attachment pads of *Tettigonia viridissima* (Orthoptera, Insecta), *J. Exper. Biol.* **203**(12), 1887−1895 (2000).

[3] Hiller, U., Untersuchungen zum Feinbau und zur Funktion der Haftborsten von Reptilien, *Z. Morphol. Tiere* **62**: 307−362 (1968).

[4] Irschick, D. J., Austin, C. C., Petren, K., Fisher, R. N., Losos, J. B., and Ellers, O. A comparative analysis of clinging ability among pad-bearing lizards. *Biol. J. Linn. Soc*. **59**: 21−35 (1996).

[5] Autumn, K., Liang, Y. A., Hsieh, S. T., Zesch, W., Chan, W. P., Kenny, T. W., Fearing, R., and Full, R. J., Adhesive force of a single gecko foot-hair, *Nature* **405**: 681−685 (2000).

[6] Autumn, K., Sitti, M., Liang, Y. A. Peattie, A. M., Hansen, W. R., Sponberg, S., Kenny, T. W., Fearing, R., Israelachvili, J. N., and Full, R. J. Evidence for van der Walls adhesion in gecko setae, *Proc. Natl. Acad. Sci. USA* **99**: 12252−12256 (2002).

[7] Arzt, E., Enders, S., and Gorb, S., Towards a micromechanical understanding of biological surface devices, *Z. Metallkd*. **93**(5): 345−351 (2002).

[8] Persson, B. N. J., On the mechanism of adhesion in biological systems, *J. Chem. Phys*. **118**: 7614−7621 (2003).

[9] Scherge, M. and Gorb, S. N., *Biological Micro- and Nanotribology*. (Springer, Berlin, 2001).

[10] Arzt, E., Gorb, S., and Spolenak, R., From micro to nano contacts in biological attachment devices, *Proc. Natl. Acad. Sci. USA* **100**: 10603−10606 (2003).

[11] Adamson, A. W., *Physical Chemistry of Surfaces*. (Wiley, Londan, 1990).

[12] Bowden, F. P., Adhäsion und Reibung, *Endeavour* **16**(61): 5−18 (1957).

[13] Johnson, K. L., Kendall, K., and Roberts, A. D., Surface energy and the contact of elastic solids, *Proc. Royal Soc. London A* **324**(1558): 301−313 (1971).

[14] Hertz, H., Über den Kontakt elastischer Körper, *J. Reine Angew. Math.* **92**: 156 (1881).

[15] Gorb, S. N., Jiao, Y., and Scherge, M., Ultrastructural architecture and mechanical properties of attachment pads in *Tettigonia viridissima* (Orthoptera Tettigoniidae), *J. Comp. Physiol.* A **186**: 821−831 (2000).

[16] Israelachvili, J., *Intermolecular & Surface Forces*, (Academic Press, London, 1992).

[17] Pisarenko, G. S., Jakovlev, A. P., and Matweev, V. V., Strength of Materials (Naukova Dumka, Kiev, 1988).

[18] Gorb, S. N. and Beutel, R. G., Evolution of locomotory attachment pads of hexapods, *Naturwissenschaften* **88**: 530−534 (2001).